

# Three Dimensional Miniaturized Super Wideband Antenna with Filtering Capabilities

Shobit Agarwal<sup>1</sup>, Ashwani Sharma<sup>1,\*</sup>, Ignacio J Garcia Zuazola<sup>2</sup>, and William G. Whittow<sup>3</sup>

<sup>1</sup>Department of Electrical Engineering, Indian Institute of Technology Ropar, Rupnagar  
Punjab, India.

<sup>2</sup>School of Computing and Digital Media, London Metropolitan University, 166-220  
Holloway Rd, London N7 8DB, United Kingdom

<sup>3</sup>Wolfson School of Mechanical, Electrical and Manufacturing Engineering, Loughborough  
University, Leicestershire, LE11 3TU, UK.

\*Corresponding Author Email: [ashwani.sharma@iitrpr.ac.in](mailto:ashwani.sharma@iitrpr.ac.in)

## Abstract

This paper presents a miniaturized three-dimensional super wideband antenna with filtering capabilities. A conventional rectangular patch antenna has been modified by truncating its corners with semi-circles and a trapezoidal shaped partial ground plane is utilized to achieve super wideband performance. The planar design is later extended to a 3D design with the addition of three dielectric cuboids in the radiator. The cuboids are inserted at low current density regions within the operating range to achieve miniaturization compared to the planar antenna. The impedance bandwidth of the 3D antenna is  $\sim 17.55$  GHz, measured from 2.45 to 20 GHz. The filtering capabilities are achieved by means of an upside-down T-shaped resonator introduced in the center of the patch and two U-shaped slots etched from the patch. In total, three interfering communication bands are rejected, WiMAX (3.2-3.8 GHz), IEEE 802.11/WLAN (5.17-5.33 GHz), and ITU (7.7-8.5 GHz). The proposed antenna is miniaturized as it merely has an overall size of  $0.20\lambda_l \times 0.19\lambda_w \times 0.011\lambda_h$  mm<sup>3</sup> (corresponds to 2.45 GHz) compared to the relevant literature. The design has been analyzed using an equivalent circuit model, fabricated and measured for validation. The simulated and measured results are found well in agreement.

## 1 Introduction

Over the last two decades, wireless communication systems have been developed at an astonishing rate. The future wireless terminals are required to bear diverse services. This prompts the need for efficient antenna systems which can function in multiple bands of the frequency spectrum. Since the allocation of Ultra-Wide Band (UWB) frequency spectrum (3.1 GHz to 10.6 GHz) by the Federal Communications Commission

(FCC) for UWB wireless communications [1], the evolution of antenna prototypes has consequently drawn attention from both academia and industry worldwide. A competent wideband antenna should be capable of operating over the entire UWB frequency and is desired to be miniaturized due to the integration requirement of the UWB systems. A universal antenna having impedance bandwidth as large as possible is always welcomed, hence, super wideband designs have evolved. Moreover, since the UWB spectrum contains various narrow bands assigned frequencies, i.e, WiMAX/5G (3.2-3.8 GHz), WLAN (5.15-5.825 GHz) and ITU (7.7-8.5 GHz) bands, interference is a major issue. Rejection of the signals in the aforementioned frequency bands is required by the universal UWB antennas. For this purpose, several planar designs have been reported [2–6] in the literature. The design approaches for achieving band rejection include etching slots of different shapes, resonators, electromagnetic band gap (EBG) structures, fractal geometries etc, on the antenna’s radiator or its or ground plane.

In [7], a multi-configuration coplanar waveguide (CPW)-fed circular antenna was designed with triple band notch characteristics. A pair of circular split ring resonators (SRRs) was incorporated at the bottom side of the antenna to achieve band notch responses at 5.24, 6.4, and 7.85 GHz. Likewise, in [8], a dual mushroom-type EBG structure was introduced at the back of a CPW-fed circular antenna, realizing rectangular notch bands for WLAN (5.15-5.8 GHz) and X-band downlink satellite communication (660 MHz, 7.10-7.76 GHz) bands. Vendik et al. [9] utilized electric ring resonators (ERRs) below the CPW feed line to achieve band notches at WiMAX (3.5 GHz and 5.8 GHz) and ITU (7.5 GHz) frequency bands. A similar type of ERR was used in [10] to reject WLAN and ITU frequency bands, where, the notch frequencies were controlled by changing the dimensions of these ERR structures. In [11], a dual-band complimentary split ring resonator (CSRR) slot was made in a rose-curve shape UWB monopole antenna to avoid interference at 3.5 GHz and 5.8 GHz. In [12], hexagonal-shaped SRRs were designed and incorporated near the feed line to provide rejection for WLAN and ITU frequency bands. In the mentioned literature, the major issues were larger antenna size, complex structures, and strong coupling effects between the band notched structures. Therefore, low complex miniature designs with largest bandwidth achievable is desired.

Etching slots in the feed line and the radiating patch is an effective technique to realise band notches. For instance, in [13], the authors used two S-shaped strips etched in the ground plane for a band-notch response at WiMAX and an elliptical ring slot (ERS) in the CPW-fed beveled patch at WLAN. In [14], a CPW-fed triangular slot antenna with dual-reverse-arrow fractal (DRAF) geometry was proposed for UWB

applications. It was shown that the use of the DRAF structure reduced the antenna size by 40%. In [15], to reject various narrow bands, U-shaped and rectangular shaped resonators were incorporated in the ground plane and a few bent U-shaped slot line like resonators of different lengths were etched on the CPW feed line. Moreover, a Fibonacci-type structure was etched within the circular patch radiator to achieve resonance at an additional GSM band.

A CPW-fed UWB antenna was presented in [16] with quadruple rejected bands; C-band (3.60-4.32 GHz), WLAN (5.17-5.32 GHz and 5.80-5.93 GHz) and ITU bands. It used, a gradient folk-shaped radiating patch with four different slots; cap-shaped slot, two meandering slots, and a split-ring, to reject the quadruple bands. In [17], a hexagonal type UWB antenna with three notched band characteristics was presented. Three C-shaped slots of different dimensions were etched in the radiating element to reject WiMAX (3.2-3.8 GHz), C-band, and WLAN (5.15-5.85 GHz) frequency bands. In [18], a fractal patch antenna was presented for UWB applications with WLAN band notch characteristics. In this design, a sectorial-circular slot was utilized to create the band notch response and the final prototype contemplated an impedance bandwidth of 11.76 GHz from 2.19 to 13.95 GHz. Further, wideband antennas with band notch characteristics were also reported in [19–22]. In these papers, the major issue was bandwidth and antenna size, reporting a maximum operating frequency of 12 GHz. Among other band notch techniques are fragment type pattern [23, 24], multiple resonator structures [25], and stub loaded antennas.

In this paper, a miniaturized three-dimensional super wideband antenna with filtering capabilities is presented. A conventional patch antenna has been modified by truncating its corners with semi-circles and by introducing a trapezoidal partial ground plane for wide impedance bandwidth over the planar design. The planar design has been extended to a 3D design with the addition of three dielectric cuboids at low current density regions within the operating range to achieve miniaturization compared to the planar antenna. That achieved an impedance bandwidth of 17.55 GHz (from 2.45 to 20 GHz) with WiMAX (3.2-3.8 GHz), IEEE 802.11/WLAN (5.17-5.33 GHz), and ITU (7.7-8.5 GHz) bands rejection in a small footprint of  $0.20\lambda_l \times 0.19\lambda_w \times 0.011\lambda_h$  mm<sup>3</sup> (at 2.45 GHz). Fabrication corroborated predictions and led to a design with a miniaturized footprint compared to other relevant literature. The proposed 3D antenna design and evolution is presented in Section 2, its equivalent circuit model in Section 3, the results, fabrication, and measurement in Section 4, and the conclusions in Section 5.

## 2 The Proposed 3D Antenna Design and Evolution

A detailed schematic of the proposed 3D triple band notch super wideband antenna is shown in Fig. 1. It uses a rectangular patch radiator with three dielectric cuboids

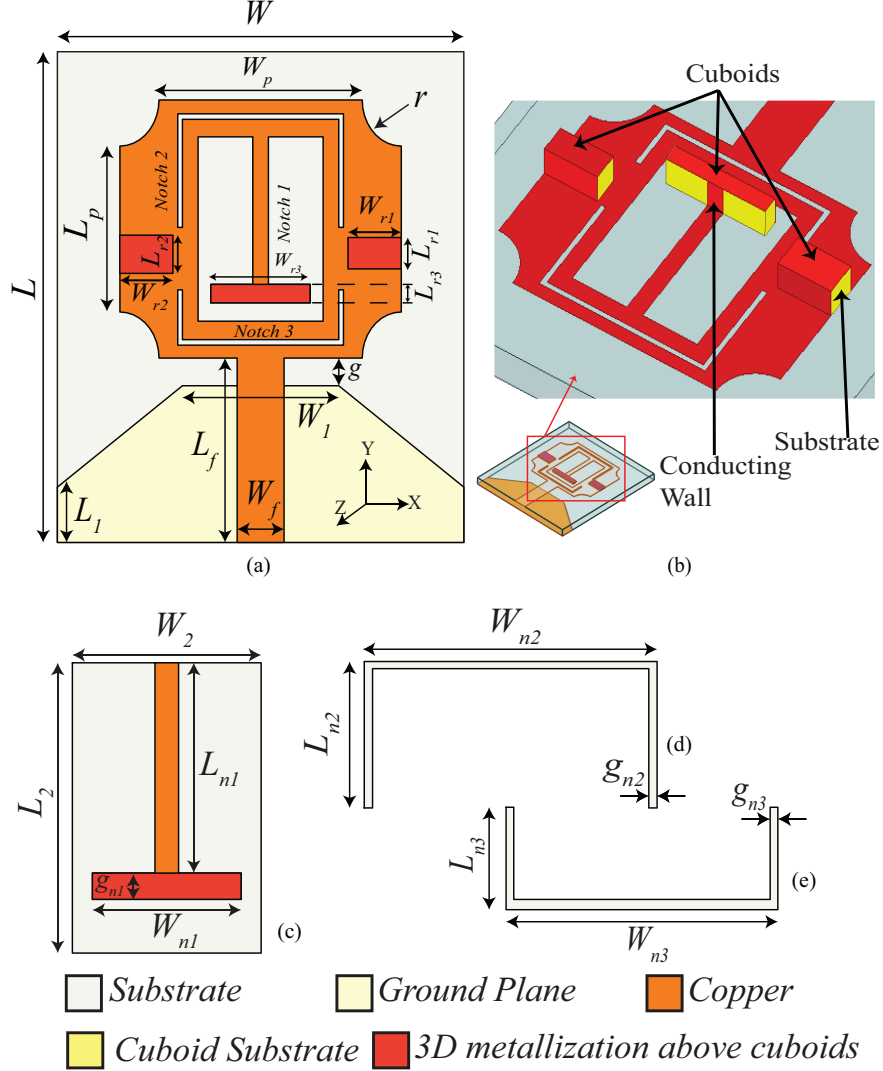


Figure 1: Schematic of the proposed 3D antenna. (a) Final antenna layout (b) perspective view in 3D (c) upside-down T-shaped resonator for WiMAX band rejection (d) upside-down U-shaped slot for WLAN band rejection (e) U-shaped slot for ITU band rejection

(Fig. 1) with 3D metallization above the cuboids and is fed by a  $50\Omega$  microstrip line over a trapezoidal partial ground plane. For band notch characteristics, a T-shaped resonator, and two U-shaped slots are etched in the radiating patch of the antenna. The proposed antenna uses Rogers RT/Duroid 5880 with dielectric constant  $\epsilon_r = 2.2$ , substrate height  $h = 1.413\text{mm}$ , substrate height of the cuboids  $h_c = 1.25\text{mm}$ , and loss tangent  $\tan \delta = 0.0009$ . The overall size of the proposed 3D antenna is  $23.4 \times 25.2$

mm<sup>2</sup> and each of its elements (dimensions) are listed in Table 1.

Table 1: Dimensions of the proposed 3D antenna (values are in mm).

Parameter	Value	Parameter	Value	Parameter	Value
$L$	28	$W_p$	13	$L_f$	10
$W$	26	$L_{n1}$	8	$W_f$	03
$L_1$	3	$W_{n1}$	6.35	$g$	1.50
$W_1$	10	$L_{n2}$	6.16	$g_{n1}$	1
$L_2$	10	$W_{n2}$	10.60	$g_{n2}$	0.30
$W_2$	8	$L_{n3}$	3	$g_{n3}$	0.30
$L_p$	9	$W_{n3}$	10.60	$r$	2.5
$W_{r1}$	3.4	$L_{r1}$	1.6	$W_{r3}$	6.35
$W_{r2}$	3.4	$L_{r2}$	2.0	$L_{r3}$	1.0
$h$	1.413	$h_c$	1.25	–	–

## 2.1 Evolution of the Proposed 3D Antenna

The advancement of the proposed 3D antenna evolves from a conventional planar rectangular patch shown in Fig. 2(a) and designated as Iteration 0. Ansys High Frequency Structure Simulator (HFSS) was used for the design study. The reflection coefficient  $S_{11}$  of Iteration 0 is shown in Fig. 3.

To improve the  $S_{11}$  below -10dB over the desired frequency band and excite other resonant modes, semi-circles of radius  $r$  were etched away from each corner of the rectangular patch. The resulting design is shown in Fig. 2(b). This is designated as Iteration 1 and used a Defected Metal Structure (DMS) technique that offered an impedance bandwidth of 17.06 GHz (from 2.94-20 GHz). However, the below -10dB was not met between 10-12 GHz.

To improve the impedance bandwidth over the entire frequency range, the partial ground plane was tailored to a trapezoidal shape. This is shown in Fig. 2(c) and designated as Iteration 2. This led to a super wideband response (Fig. 3) with an impedance bandwidth of 17.29 GHz from 2.71-20 GHz according to  $S_{11} \leq -10$ dB.

### 2.1.1 Single Notch Insertion

The major issue in designing a band-notch antenna is the placement of specific structures in the antenna for band rejection. For single band notch, an upside-down T-shaped resonator was introduced; this is shown in Fig. 2(d) and designated as Itera-

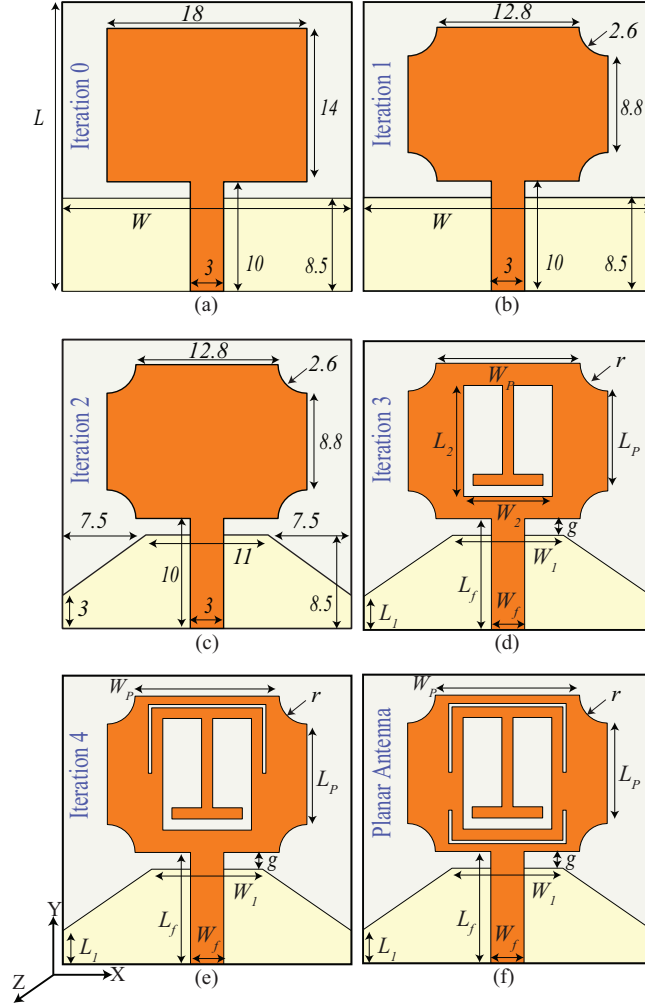


Figure 2: Design evolution. (values are in mm) (a) Iteration 0: a conventional rectangular patch with partial ground plane. (b) Iteration 1: Etched corners with semi-circles. (c) Iteration 2: Tailored partial ground plane to a trapezoidal shape (d) Iteration 3: Upside-down T-shaped resonator for WiMAX band rejection (e) Iteration 4: Upside-down U-shaped resonator for WLAN band rejection (f) Planar antenna: U-shaped resonator for ITU band rejection.

tion 3. The optimized dimensions of the T-shaped resonator (Fig. 1(c)) are given in Table 1. The overall length of the T-shaped resonator is equal to  $\lambda_g/4$ , where  $\lambda_g$  is the guided wavelength at 3.5 GHz. The simulated  $S_{11}$  response of the Iteration 3 is given in Fig. 4(a) and showed a band-notch from 3.49 to 3.76 GHz centered at 3.64 GHz without adversely impacting on the super wideband performance except the rejected band.

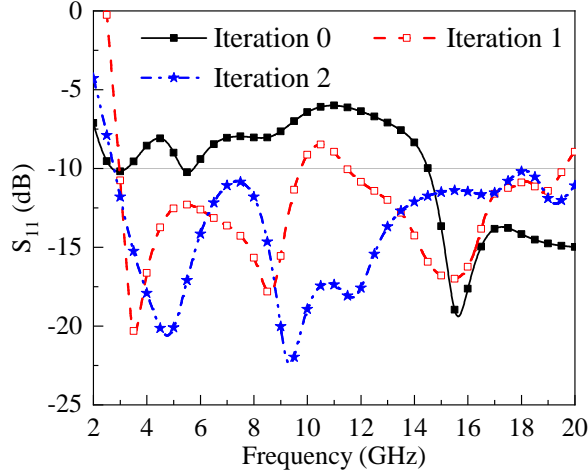


Figure 3: Simulated  $S_{11}$  of iterations, 0 to 2.

### 2.1.2 Dual Notch Insertion

The second notch is achieved by etching an upside-down U-shaped slot (resonator) in the radiating element of the antenna (Fig. 2(e)) and is designated as Iteration 4. The length of the inverted U-shaped slot (resonator) [26] is calculated using (1),

$$L_s = \frac{c}{2f_r\sqrt{\varepsilon_{reff}}} \quad , \quad \varepsilon_{reff} = \frac{\varepsilon_r + 1}{2}, \quad (1)$$

where  $L_s = 2L_n + W_n$  is the total length of the slot,  $f_r$  corresponds to the resonant frequency, and  $\varepsilon_r$  the relative permittivity of the dielectric substrate. In Fig. 4(a), the simulated  $S_{11}$  of Iteration 4 is presented and showed a band notch from 5.15 to 5.27 GHz centered at 5.2 GHz. It was observed that the upside-down U-shaped slot (resonator), existing in the vicinity of the T-shaped resonator, affected positively the first notch response (Fig. 4(a)). As a result, the frequency of the lower notch downshifted 60 MHz leading to a band notch from 3.43 to 3.62 GHz centered at 3.51 GHz which was sufficient to reject the undesired WiMAX band.

### 2.1.3 Triple Notch Insertion

A third notch prevented interference from the dedicated bands of down-link of X-band and satellite communication as per the specifications of ITU. For this, another U-shaped slot (resonator) of dimensions  $L_{n3} \times W_{n3}$  mm<sup>2</sup> was etched in the radiating element of the antenna, Fig. 2(f) and is designated as the planar antenna. The total length of the U-shaped slot (resonator) was initially calculated using (1) and tuned subsequently for the desired  $S_{11}$  parameter; the simulated response is shown in Fig. 4(a) where the three desired notch bands are visible. Since this U-shaped slot

(resonator) was wrapped around the T-shaped resonator, a downshift of 60 MHz was observed. That let the final notch bands lie in the frequency range of 3.37-3.60 GHz, 5.16- 5.30 GHz, and 7.17-8.77 GHz.

The gain responses of Iteration 2, 3, 4 and planar antenna are shown in Fig. 4(b). From the figure, it can be observed that the gain of the antenna decreases (drops below 0dBi) within the notch bands which confirms minimal radiation for the rejected bands.

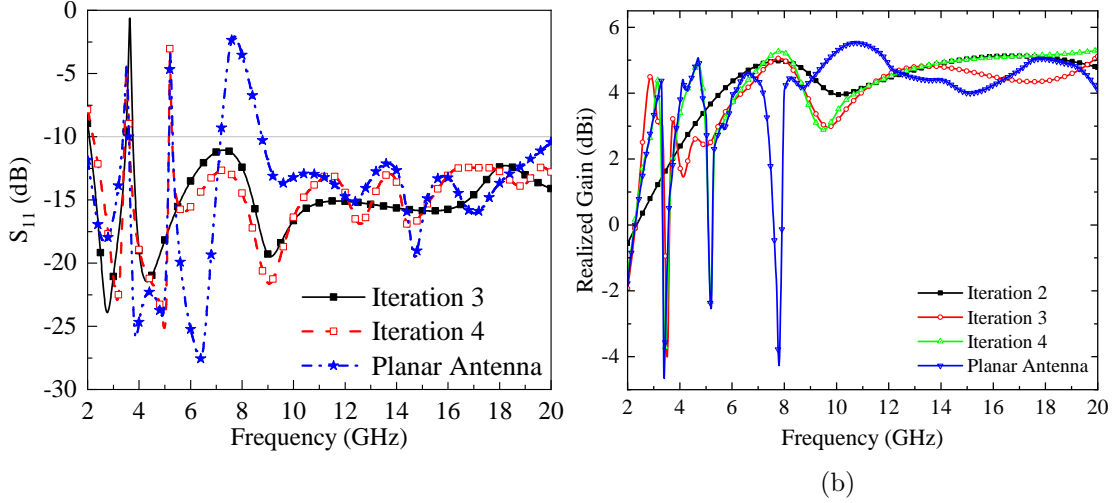


Figure 4: Simulated (a)  $S_{11}$  of iterations 3, 4 and the planar antenna (b) gain response of Iterations 2, 3, 4 and the planar antenna.

## 2.2 Insertion of the Dielectric Cuboids

In an attempt to miniaturize the planar antenna, the maximum current densities mapped over the entire operating range (2.45 GHz - 20 GHz), by superimposing the current density at different frequencies is shown in Fig. 5. The merged profile was analyzed and found common areas where low currents exist and since strong magnetic fields are present in the center of a patch [27, 28], the planar design was extended to a 3D design with the addition of three dielectric cuboids where low current density regions exist and the magnetic field is strong there. This is shown in Fig. 1 and is designated as the proposed 3D antenna, with cuboid dimensions summarized in Table 1.

However, the insertion of these cuboid slanted the planar antenna  $S_{11}$  response (Fig. 4). To overcome this, a parametric study was conducted on the cuboids height ( $h_c$ ) to optimize the performance. The simulated  $S_{11}$  responses for different values of  $h_c$  is shown in Fig. 6(a). It is evident from the figure that the frequency response downshifted with increasing  $h_c$ .

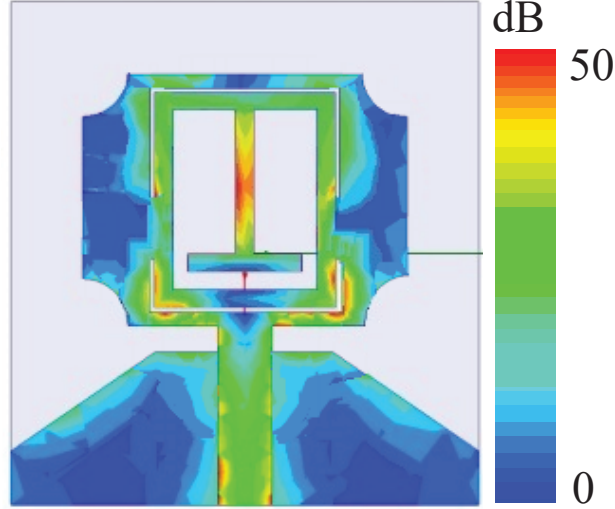


Figure 5: Maximum current densities of the planar antenna mapped over the entire operating frequency range (2.45 to 20 GHz).

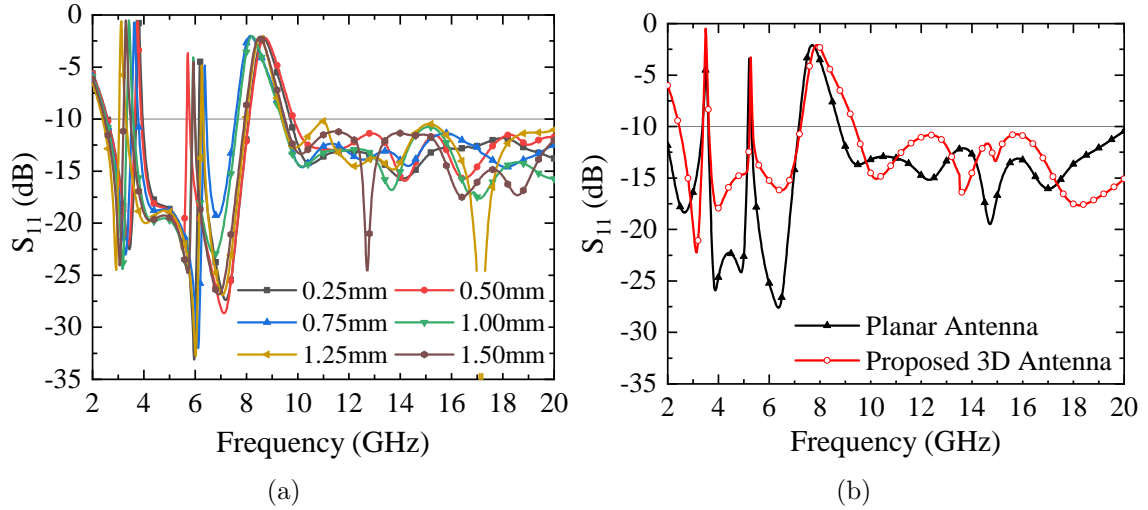


Figure 6: Simulated (a)  $S_{11}$  responses for different values of  $h_c$  (b)  $S_{11}$  responses of the proposed 3D antenna compared to the planar antenna.

The optimal value of  $h_c$  was found to be 1.25mm and that allowed the overall dimensions of the antenna to be reduced by 10% which led to a proposed 3D antenna of  $25.2 \times 23.4 \times 1.413 \text{ mm}^3$  ( $0.20\lambda_l \times 0.19\lambda_w \times 0.011\lambda_h$ ; corresponds to 2.45 GHz). Therefore, the proposed 3D antenna was miniaturized by 27.1% when compared to the size of the planar antenna.. The simulated  $S_{11}$  responses of both antennas, the 3D compared to the planar, are shown in Fig. 6(b). Because the miniaturization of the antenna and related up-shift frequency, the proposed 3D antenna showed comparable  $S_{11}$  response with notch bands laying within 3.39-3.64 GHz, 5.16-5.36 GHz, and 7.26-9.38 GHz.

### 3 Equivalent Circuit Model Analysis of the Antenna

For ease of analysis and tuning of the antenna, an equivalent circuit model was devised. This is important since most of the RF front-end components are analyzed in time domain simulators. Fig. 7 shows the equivalent circuit model of the antenna. To account for the impedance of a super wideband antenna, Foster canonical form

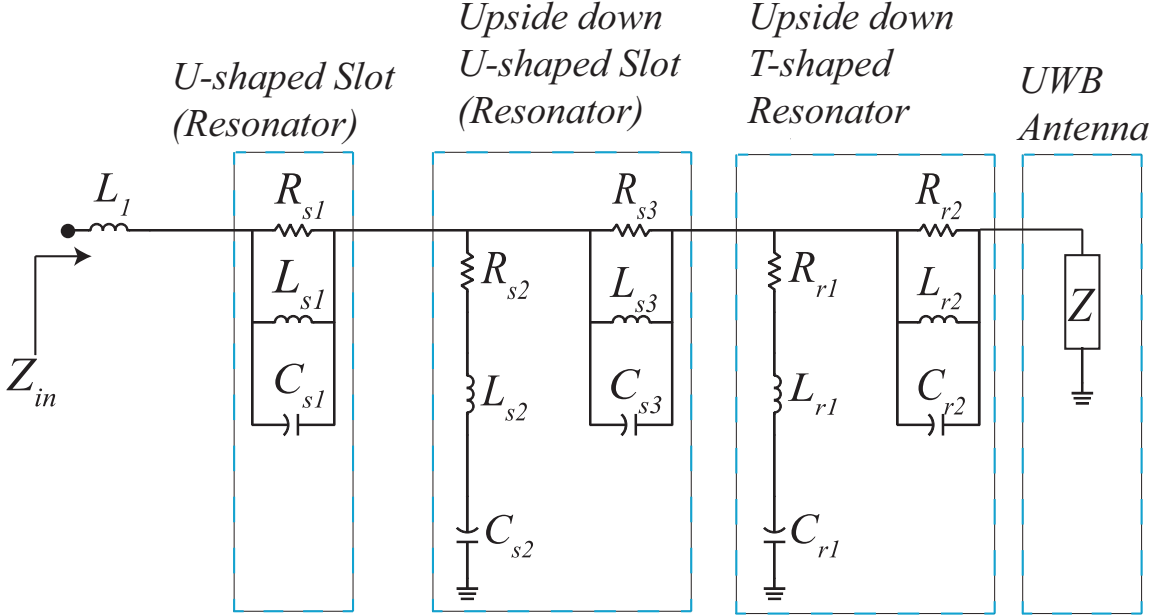


Figure 7: Equivalent lumped element model of the antenna.

technique was utilized where each mode of the antenna was represented by a series of parallel RLC circuits [29]. To calculate the values of the RLC components of the circuit, the equivalent impedance,  $Z_{eq}$ , is utilized and calculated as:

$$Z_{eq} = \sum_{k=1}^n \frac{j\omega R_k L_k}{R_k(1 - \omega^2 L_k C_k) + j\omega L_k}. \quad (2)$$

For simplification, only the real part of (2) is considered and calculated as:

$$R_{eq} = \sum_{k=1}^n \frac{R_k}{1 + R_k \left( \frac{1}{2\pi f L_k} - 2\pi f C_k \right)^2}. \quad (3)$$

After inputting the data values obtained from the HFSS electromagnetic (EM) simulator in eq.3, values of the RLC components were found using an iterative method [30]. Furthermore, the U-shaped slots (resonators) and T-shaped resonator were modeled

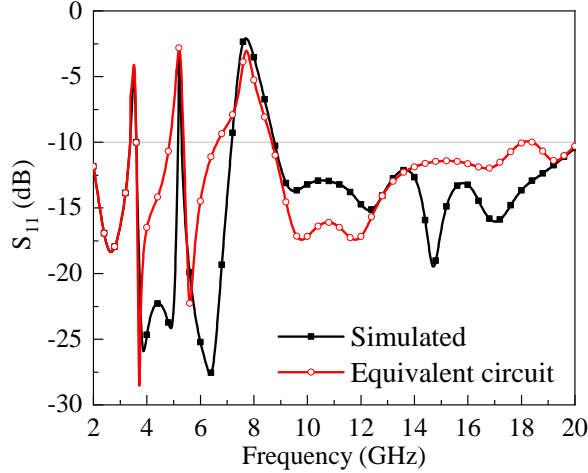


Figure 8: Comparison of the antenna performance, simulated vs. equivalent circuit.

as a combination of series and parallel RLC (Fig. 7). The upside-down T-shaped resonator and upside-down U-shaped slot (resonator) were modeled using a combination of series and parallel RLC, whereas the U-shaped slot (resonator) was modeled as a parallel RLC. The equivalent lumped element model of Fig. 7 was simulated using Agilent ADS. The equivalent circuit parameters are summarized in Table 2. Fig. 8 shows the comparison of the antenna performance, simulated vs. equivalent circuit with fair agreement validating the equivalent circuit model analysis.

Table 2: Optimized value of equivalent circuit model of the proposed antenna

Parameter	Value	Parameter	Value	Parameter	Value	Parameter	Value
$L_1$	0.05 nH	$R_{r2}$	0.15 k $\Omega$	$L_{r1}$	150 nH	$C_{s3}$	9.3 pF
$R_{s1}$	0.2 k $\Omega$	$L_{s1}$	0.1 nH	$L_{r2}$	0.11 nH	$C_{r1}$	10 pF
$R_{s2}$	10 $\Omega$	$L_{s2}$	150 nH	$C_{s1}$	4.27 pF	$C_{r2}$	18.4 pF
$R_{r1}$	10 $\Omega$	$L_{s3}$	0.1 nH	$C_{s2}$	10 pF	—	

## 4 Results, Fabrication, and Measurement

The surface maximum current distributions of the planar antenna at the three notch frequencies are shown in Fig. 9. It is observed that for 3.5 GHz, the current was concentrated around the T-shaped resonator, whereas, for 5.25 GHz and 7.7 GHz, the current majorly lies around the corresponding U-shaped slots (resonators). This specifies that at these frequencies, there is almost negligible radiations from the antenna [31].

The simulated and measured  $S_{11}$  results of the planar antenna are presented in Fig. 10. The fabricated prototype is shown in the inset of Fig. 10, which is characterized

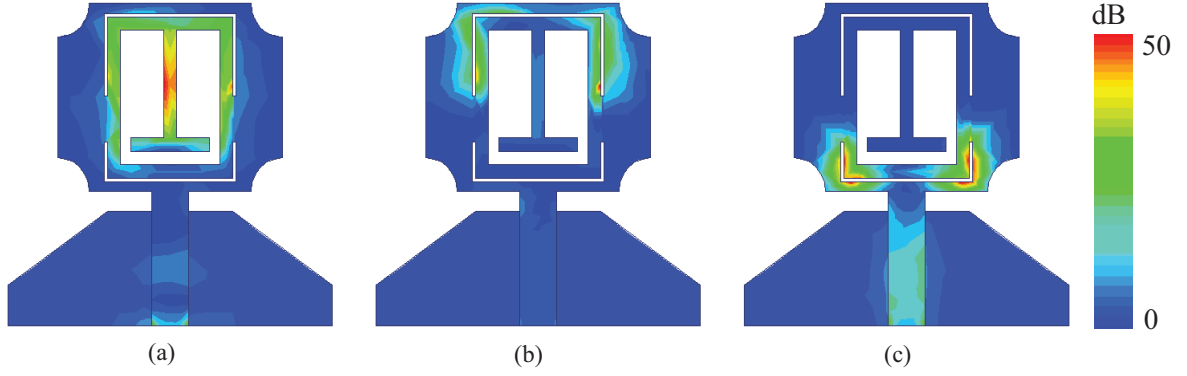


Figure 9: Simulated maximum current distribution at different notch frequencies of the planar antenna. (a) 3.5 GHz (b) 5.2 GHz (c) 7.7 GHz

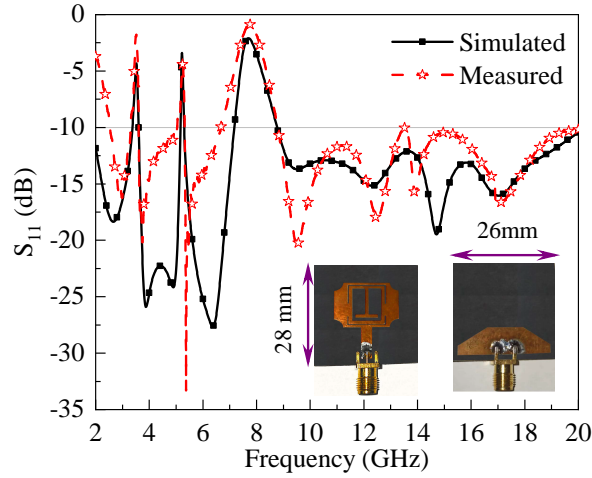


Figure 10: Simulated and measured  $S_{11}$  response of the planar antenna (front and back of the fabricated prototype are shown as inset).

using Agilent Technologies Power Network Analyzer (PNA-L) N5234B in the frequency range of 2-20 GHz. It was noted that the simulated and measured  $S_{11}$  results (Fig. 10) are in fair agreement and the discrepancies were due to fabrication tolerances. The fabricated prototype for the front and back of the proposed 3D is shown in Fig. 11(a) and (b), respectively. The simulated and measured  $S_{11}$  responses of the proposed 3D antenna are shown in Fig. 11(c) with reasonable agreement between the results.

The simulated (Co- and Cross-polar) and measured (Co-polar) E- and H-plane (correspond to the XZ and YZ planes of Fig. 1 (a), respectively) radiation patterns of the planar and the proposed 3D antenna at frequencies 3 GHz, 9 GHz, and 15 GHz are depicted in Fig. 12 and Fig. 13, respectively.

For 3 GHz and 9 GHz as shown in Fig. 12(a, b), a monopole like radiation pattern was observed in the E-plane and an omnidirectional radiation in the H-plane. For 15

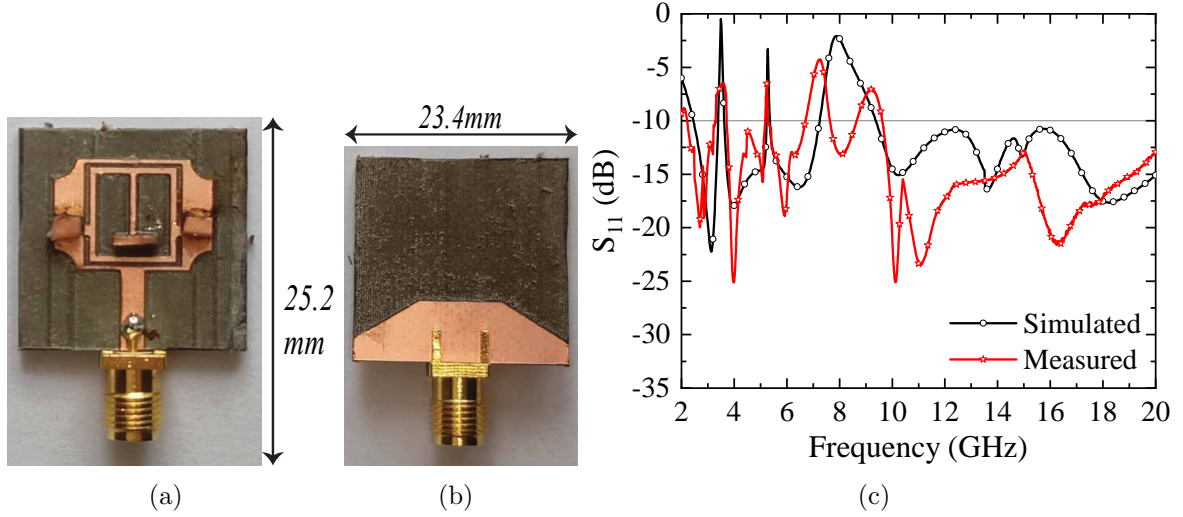


Figure 11: The (a) front and (b) back of the fabricated prototype; (c) the simulated and measured  $S_{11}$  response of the proposed 3D antenna.

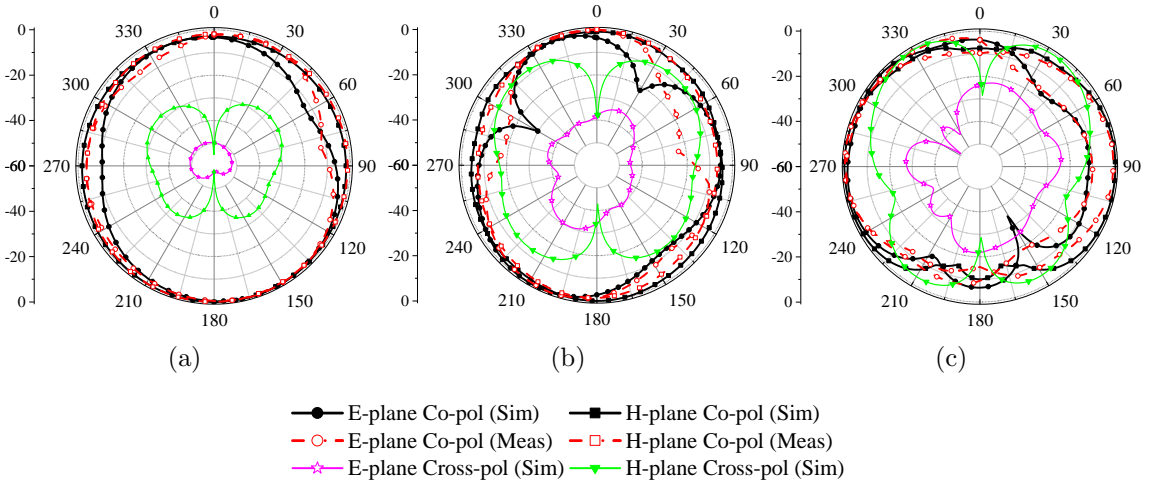


Figure 12: Simulated (Co- and Cross-polar) and measured (Co-polar) normalized radiation patterns of the planar antenna at (a) 3 GHz (b) 9 GHz (c) 15 GHz

GHz as shown in Fig. 12(c), less omnidirectional radiation patterns were observed in both of the planes. Similarly, from Fig. 13(a-c), the radiation patterns were in coherence with those of the planar antenna (Fig. 11) and thus the radiation performance of the antenna did not present any significant alteration with the presence of the cuboids.

The simulated and measured realized gain of the proposed 3D antenna is shown in Fig. 14. Results showed reasonable agreement with those simulated, and that the proposed 3D antenna increased its gain with frequency. Nevertheless, sharp gain reductions were met at the three notched bands which signifies the validation of the design. The simulated and measured peak gains of the proposed 3D antenna were 5.67

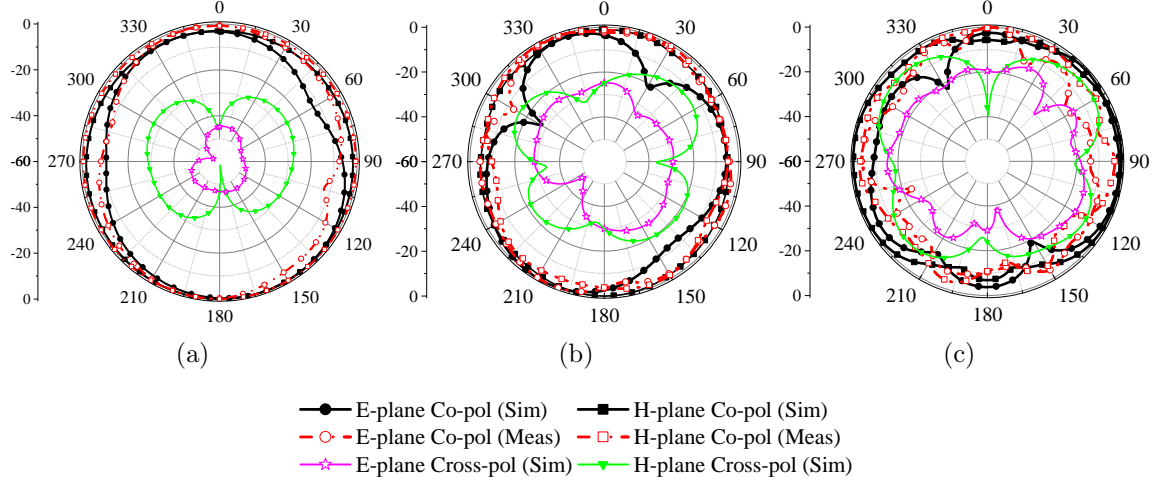


Figure 13: Simulated (Co- and Cross-polar) and measured (Co-polar) normalized radiation patterns of the proposed 3D antenna at (a) 3 GHz (b) 9 GHz (c) 15 GHz

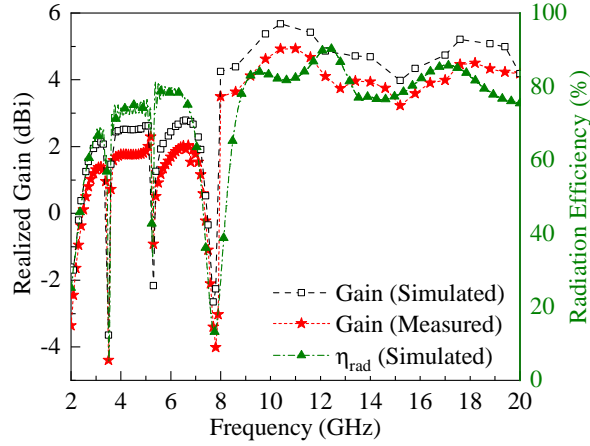


Figure 14: Simulated and measured realized gain and simulated radiation efficiency of the proposed 3D antenna.

dBi and 4.93 dBi respectively at 10.4 GHz.

Table 3 gives a comparison of the proposed 3D antenna with other relevant super wide band notch antennas in the literature. From the comparative data, the proposed antenna provided better fractional bandwidth (FBW) with small footprint at a relatively high gain compared to the other literature [7–9, 11, 12, 15, 17, 19–22, 31–37] while offering triple notched band characteristics with good notched band response. It is for this reason the proposed antenna is termed as miniature.

Table 3: Comparison of the proposed 3D antenna with other relevant super wide band notch antennas in the literature.

Ref.	Operating frequency (GHz)	Size ( $\lambda_l \times \lambda_w$ )	Size (mm×mm)	Fractional Bandwidth (FBW) (%)	Peak Realized Gain (dBi)	Notch Bands (GHz)
[7]	2.6 - 10.8	0.43×0.61	50×70	122	4.0	5.09; 6.34; 8.04
[8]	2.66 - 11	0.43×0.44	48×50	122	5.1	5.15-5.82; 7.1-7.76
[9]	2.5 - 12	0.42×0.42	50×50	131	5.0	3.5; 5.8; 7.5
[11]	3.1 - 11	0.35×0.36	34×35	112	5.7	3.48-3.95; 5.5-5.92
[12]	2.8 - 11	0.28×0.37	30×40	119	6.0	5.8; 6.8
[15]	3.2 - 11.9	0.58×0.59	54×55	115	10.2	3.06-3.54; 3.59-4.86; 5.93-7.15
[17]	2.95 - 12	0.30×0.29	30×30	121	5.4	3.2-3.85; 4.05-4.45; 5.1-5.9
[19]	3 - 11	0.48×0.46	48×46	114	5.9	4.9-6.3
[20]	2.7 - 10.8	0.41×0.36	45×40	120	5.9	3.5-4.35; 5.05-5.95
[21]	2.5 - 12	0.40×0.40	48×48	131	7.0	5.1-6
[22]	3.4 - 12	0.45×0.45	40×40	112	6.7	5-5.9; 7.2-8
[31]	2.6 - 23	0.35×0.30	40×35	159	7.8	3.1-4.45; 5.15-6.30; 8.45-9.05
[32]	3.1 - 10.6	0.28×0.32	27×30.5	109	4.0	3.36-3.88; 4.96-6.23; 7.9-8.7
[33]	1.42 - 50	0.27×0.16	57×34	119	7.0	3.4; 5.6; 9
[34]	2.15 - 15	0.20×0.22	28×30	149.8	1.75	3.3-3.7; 3.8-4.2; 5.2-5.8
[35]	2.5 - 12	0.33×0.25	40×30	131	2.55	3.5
[36]	3.1 - 10	0.36×0.36	35×35	105.3	6.0	3.39; 5.78; 8.60
[37]	3 - 12	0.30×0.30	30×30	120	2.0	3.2-3.8; 4.05-4.45; 5.1-5.9
[38]	1.6-47.5	0.24×0.21	45×40	187	5	1.8-4.2; 4.7-2; 9.8-10.4
Planar antenna	2.71 - 20	0.25×0.23	28×26	152.27	5.67	3.37-3.6; 5.16-5.30; 7.17-8.77
Proposed 3-D antenna	2.45 - 20	0.20×0.19	25.2×23.4	156	5.0	3.39-3.64; 5.16-5.36; 7.26-9.38

where,  $\lambda_l$  and  $\lambda_w$  are normalized length and width (in wavelengths) corresponding to the lowest operating frequency.

## 5 Conclusion

A miniaturized three-dimensional super wideband antenna with filtering capabilities has been presented. A conventional patch antenna was modified by truncating its corners with semi-circles and by introducing a trapezoidal partial ground plane for wide impedance bandwidth over a planar design. The planar design was extended to a 3D design with the addition of three dielectric cuboids at low current density regions within the operating range to achieve miniaturization compared to the planar antenna. That achieved a super wide impedance bandwidth of 17.55 GHz (from 2.45 to 20 GHz) mainly attributed to the tailored trapezoidal partial ground plane with WiMAX (3.2-3.8 GHz), IEEE 802.11/WLAN (5.17-5.33 GHz), and ITU (7.7-8.5 GHz) bands rejection by incorporating three notched band resonators in the radiating element of the antenna and was analytically studied using an equivalent circuit model for its validation. With the addition of the three dielectric cuboids, the overall dimensions of the antenna were reduced by 10%. That compared to the planar antenna was a 27.1% smaller footprint. Fabrication corroborated predictions and led to a proposed 3D antenna design with a miniature footprint of  $25.2 \times 23.4 \times 1.413 \text{ mm}^3$  ( $0.20\lambda_l \times 0.19\lambda_w \times 0.011\lambda_h$  at 2.45 GHz) compared to other relevant literature. The proposed antenna can be utilized for many wireless applications such as Wi-Fi/WLAN,

WiMAX, radar communications, satellite and defense communication, wireless access systems (WAS)/radio local area networks (RLANS) (17.1–17.3 GHz), broadband disaster relief (BBDR) (4.94–4.99 GHz), radio determination applications (4.5–7 GHz, 13.4–14 GHz).

## 6 Acknowledgements

This work is supported in part by Department of Science and Technology (DST), Science and Engineering Research Board (SERB), Government of India under grant ECR/2018/000343 and the United Kingdom EPSRC grant (EP/S030301/1).

## References

- [1] FCC, “Revision of part 15 of the commission’s rules regarding ultra-wideband transmission systems, First note and order,” 2002.
- [2] C. M. Dikmen, S. Cimen, and G. Çakır, “Planar octagonal-shaped UWB antenna with reduced radar cross section,” *IEEE Transactions on Antennas and Propagation*, vol. 62, no. 6, pp. 2946–2953, 2014.
- [3] H. Malekpoor and S. Jam, “Analysis on bandwidth enhancement of compact probe-fed patch antenna with equivalent transmission line model,” *IET Microwaves, Antennas & Propagation*, vol. 9, no. 11, pp. 1136–1143, 2015.
- [4] M. G. N. Alsath and M. Kanagasabai, “Compact UWB monopole antenna for automotive communications,” *IEEE Transactions on Antennas and Propagation*, vol. 63, no. 9, pp. 4204–4208, 2015.
- [5] D. Zhao, C. Yang, M. Zhu, and Z. Chen, “Design of WLAN/LTE/UWB antenna with improved pattern uniformity using ground-cooperative radiating structure,” *IEEE Transactions on Antennas and Propagation*, vol. 64, no. 1, pp. 271–276, 2015.
- [6] M. N. Shakib, M. Moghavvemi, and W. N. Mahadi, “A low-profile patch antenna for ultrawideband application,” *IEEE Antennas and Wireless Propagation Letters*, vol. 14, pp. 1790–1793, 2015.
- [7] L. A. Shaik, C. Saha, J. Y. Siddiqui, and Y. M. Antar, “Ultra-wideband monopole antenna for multiband and wideband frequency notch and narrowband applica-

- tions,” *IET Microwaves, Antennas & Propagation*, vol. 10, no. 11, pp. 1204–1211, 2016.
- [8] L. Peng, B.-J. Wen, X.-F. Li, X. Jiang, and S.-M. Li, “CPW fed UWB antenna by EBGs with wide rectangular notched-band,” *IEEE Access*, vol. 4, pp. 9545–9552, 2016.
- [9] I. B. Vendik, A. Rusakov, K. Kanjanasit, J. Hong, and D. Filonov, “Ultrawideband (UWB) planar antenna with single-, dual-, and triple-band notched characteristic based on electric ring resonator,” *IEEE Antennas and Wireless Propagation Letters*, vol. 16, pp. 1597–1600, 2017.
- [10] A. Gorai and R. Ghatak, “Multimode resonator-assisted dual band notch UWB antenna with additional bluetooth resonance characteristics,” *IET Microwaves, Antennas & Propagation*, vol. 13, no. 11, pp. 1854–1859, 2019.
- [11] O. A. Safa, M. Nedil, L. Talbi, and K. Hettak, “Coplanar waveguide-fed rose-curve shape UWB monopole antenna with dual-notch characteristics,” *IET Microwaves, Antennas & Propagation*, vol. 12, no. 7, pp. 1112–1119, 2018.
- [12] K. Fertas, F. Ghanem, A. Azrar, and R. Aksas, “UWB antenna with sweeping dual notch based on metamaterial SRR fictive rotation,” *Microwave and Optical Technology Letters*, vol. 62, no. 2, pp. 956–963, 2020.
- [13] S. R. Emadian and J. Ahmadi-Shokouh, “Very small dual band-notched rectangular slot antenna with enhanced impedance bandwidth,” *IEEE Transactions on Antennas and Propagation*, vol. 63, no. 10, pp. 4529–4534, 2015.
- [14] H. Soleimani and H. Orazi, “Miniaturization of UWB triangular slot antenna by the use of dual-reverse-arrow fractal,” *IET, Microwave, Antennas and Propagation*, pp. 1–13, 2016.
- [15] K. Srivastava, A. Kumar, B. K. Kanaujia, S. Dwari, A. K. Verma, K. P. Esselle, and R. Mittra, “Integrated GSM-UWB fibonacci-type antennas with single, dual, and triple notched bands,” *IET Microwaves, Antennas & Propagation*, vol. 12, no. 6, pp. 1004–1012, 2018.
- [16] Z.-P. Zhong, J.-J. Liang, M.-L. Fan, G.-L. Huang, W. He, X.-C. Chen, and T. Yuan, “A compact CPW-fed UWB antenna with quadruple rejected bands,” *Microwave and Optical Technology Letters*, vol. 61, no. 12, pp. 2795–2800, 2019.

- [17] B. Hammache, A. Messai, I. Messaoudene, and T. A. Denidni, “A compact ultra-wideband antenna with three C-shaped slots for notched band characteristics,” *Microwave and Optical Technology Letters*, vol. 61, no. 1, pp. 275–279, 2019.
- [18] R. K. Garg, M. V. D. Nair, S. Singhal, and R. Tomar, “A new type of compact ultra-wideband planar fractal antenna with WLAN band rejection,” *Microwave and Optical Technology Letters*, vol. 62, no. 7, pp. 2537–2545, 2020.
- [19] Y.-S. Hu, M. Li, G.-P. Gao, J.-S. Zhang, and M.-K. Yang, “A double-printed trapezoidal patch dipole antenna for UWB applications with band-notched characteristic,” *Progress In Electromagnetics Research*, vol. 103, pp. 259–269, 2010.
- [20] A. A. Kalteh, G. DadashZadeh, and M. Naser-Moghadasi, “Implementation and investigation of circular slot UWB antenna with dual-band-notched characteristics,” *EURASIP Journal on Wireless Communications and Networking*, vol. 2011, no. 1, p. 88, 2011.
- [21] P. Gao, S. He, X. Wei, Z. Xu, N. Wang, and Y. Zheng, “Compact printed UWB diversity slot antenna with 5.5-GHz band-notched characteristics,” *IEEE Antennas and Wireless Propagation Letters*, vol. 13, pp. 376–379, 2014.
- [22] J. Zhu, B. Feng, B. Peng, S. Li, and L. Deng, “Compact CPW UWB diversity slot antenna with dual band-notched characteristics,” *Microwave and Optical Technology Letters*, vol. 58, no. 4, pp. 989–994, 2016.
- [23] Y. Du, X. Wu, J. Sidén, and G. Wang, “Design of sharp roll-off band notch with fragment-type pattern etched on UWB antenna,” *IEEE Antennas and Wireless Propagation Letters*, vol. 17, no. 12, pp. 2404–2408, 2018.
- [24] Y. Du, X. Wu, J. Sidén, and G. Wang, “Design of ultra-wideband antenna with high-selectivity band notches using fragment-type etch pattern,” *Microwave and Optical Technology Letters*, vol. 62, no. 2, pp. 912–918, 2020.
- [25] J. Zhang, P. Cao, Y. Huang, R. Alrawashdeh, and X. Zhu, “Compact planar ultra-wideband antenna with quintuple band-notched characteristics,” *IET Microwaves, Antennas & Propagation*, vol. 9, no. 3, pp. 206–216, 2014.
- [26] C. A. Balanis, *Antenna theory: analysis and design*. John wiley & sons, 2016.
- [27] A. Motevasselian and W. G. Whittow, “Miniaturization of a circular patch microstrip antenna using an arc projection,” *IEEE Antennas and Wireless Propagation Letters*, vol. 16, pp. 517–520, 2016.

- [28] I. J. G. Zuazola, A. Sharma, M. Filip, and W. G. Whittow, "Antenna using a magnetic-slab located in the principal magnetic-field region beneath the patch," *Progress In Electromagnetics Research C*, vol. 110, pp. 229–241, 2021.
- [29] Q.-X. Chu and Y.-Y. Yang, "A compact ultrawideband antenna with 3.4/5.5 GHz dual band-notched characteristics," *IEEE Transactions on Antennas and Propagation*, vol. 56, no. 12, pp. 3637–3644, 2008.
- [30] I. Pele, A. Chousseaud, and S. Toutain, "Simultaneous modeling of impedance and radiation pattern antenna for UWB pulse modulation," in *IEEE Antennas and Propagation Society Symposium, 2004.*, vol. 2. IEEE, 2004, pp. 1871–1874.
- [31] W. H. A. Al Amro and M. K. Abdelazeez, "Analysis and optimisation of super-wideband monopole antenna with tri-band notch using a transmission line model," *IET Microwaves, Antennas & Propagation*, vol. 13, no. 9, pp. 1373–1381, 2019.
- [32] Y.-Z. Cai, H.-C. Yang, and L.-Y. Cai, "Wideband monopole antenna with three band-notched characteristics," *IEEE Antennas and Wireless Propagation Letters*, vol. 13, pp. 607–610, 2014.
- [33] X. Zhang, S. Ur Rahman, Q. Cao, I. Gil *et al.*, "A novel SWB antenna with triple band-notches based on elliptical slot and rectangular split ring resonators," *Electronics*, vol. 8, no. 2, p. 202, 2019.
- [34] S. Vijay, M. Ahmad, B. Ahmad, S. Rawat, P. Singh, K. Ray, and A. Bandyopadhyay, "Designing of UWB monopole antenna with triple band notch characteristics at WiMAX/C-Band/WLAN," in *Proceedings of International Conference on Data Science and Applications*. Springer, 2021, pp. 123–131.
- [35] N. Ahuja, R. Khanna, and J. Kaur, "Infinite length slotted ultra-wideband monopole antenna using step-feed with band notch characteristics," *International Journal of Microwave and Wireless Technologies*, pp. 1–8, 2021.
- [36] V. R. Kapure, P. P. Bhavarthe, and S. S. Rathod, "Tunable triple band-notched UWB antenna using single EBG and varactor diode," *Progress In Electromagnetics Research C*, vol. 110, pp. 181–195, 2021.
- [37] A. A. Kadam and A. A. Deshmukh, "Modal analysis of triple band notch ultra-wideband antenna with three C-shaped slots," in *2021 International Conference on Communication information and Computing Technology (ICCICT)*. IEEE, 2021, pp. 1–4.

- [38] W. Balani, M. Sarvagya, T. Ali, A. Samasgikar, S. Das, P. Kumar, and J. Anguera, “Design of SWB antenna with triple band notch characteristics for multipurpose wireless applications,” *Applied Sciences*, vol. 11, no. 2, p. 711, 2021.